



**HAL**  
open science

## Construction of merged satellite total O<sub>3</sub> and NO<sub>2</sub> time series in the tropics for trend studies and evaluation by comparison to NDACC SAOZ measurements

Maud Pastel, Jean-Pierre Pommereau, Florence Goutail, A. Richter, Andrea Pazmino, Dmitry V. Ionov, Thierry Portafaix

### ► To cite this version:

Maud Pastel, Jean-Pierre Pommereau, Florence Goutail, A. Richter, Andrea Pazmino, et al.. Construction of merged satellite total O<sub>3</sub> and NO<sub>2</sub> time series in the tropics for trend studies and evaluation by comparison to NDACC SAOZ measurements. *Atmospheric Measurement Techniques*, 2014, 7, pp.3337-3354. 10.5194/amt-7-3337-2014 . hal-00829176

**HAL Id: hal-00829176**

**<https://hal.science/hal-00829176>**

Submitted on 28 Dec 2015

**HAL** is a multi-disciplinary open access archive for the deposit and dissemination of scientific research documents, whether they are published or not. The documents may come from teaching and research institutions in France or abroad, or from public or private research centers.

L'archive ouverte pluridisciplinaire **HAL**, est destinée au dépôt et à la diffusion de documents scientifiques de niveau recherche, publiés ou non, émanant des établissements d'enseignement et de recherche français ou étrangers, des laboratoires publics ou privés.



# Construction of merged satellite total O<sub>3</sub> and NO<sub>2</sub> time series in the tropics for trend studies and evaluation by comparison to NDACC SAOZ measurements

M. Pastel<sup>1</sup>, J.-P. Pommereau<sup>1</sup>, F. Goutail<sup>1</sup>, A. Richter<sup>2</sup>, A. Pazmiño<sup>1</sup>, D. Ionov<sup>3</sup>, and T. Portafaix<sup>4</sup>

<sup>1</sup>Laboratoire Atmosphères, Milieux, Observations Spatiales, CNRS, UMR8190, Université Versailles Saint Quentin, Guyancourt, France

<sup>2</sup>Institute of Environmental Physics, University of Bremen, Bremen, Germany

<sup>3</sup>Research Institute of Physics, St. Petersburg State University, St. Petersburg, Russia

<sup>4</sup>Laboratoire de l'Atmosphère et des Cyclones, UMR8105, CNRS – Université de la Réunion – Météo-France, Saint Denis de la Réunion, France

Correspondence to: M. Pastel (maud.pastel@latmos.ipsl.fr)

Received: 2 May 2013 – Published in Atmos. Meas. Tech. Discuss.: 31 May 2013

Revised: 28 June 2014 – Accepted: 22 August 2014 – Published: 7 October 2014

**Abstract.** Long time series of ozone and NO<sub>2</sub> total column measurements in the southern tropics are available from two ground-based SAOZ (Système d'Analyse par Observation Zénithale) UV-visible spectrometers operated within the Network for the Detection of Atmospheric Composition Change (NDACC) in Bauru (22° S, 49° W) in S-E Brazil since 1995 and Reunion Island (21° S, 55° E) in the S-W Indian Ocean since 1993. Although the stations are located at the same latitude, significant differences are observed in the columns of both species, attributed to differences in tropospheric content and equivalent latitude in the lower stratosphere. These data are used to identify which satellites operating during the same period, are capturing the same features and are thus best suited for building reliable merged time series for trend studies. For ozone, the satellites series best matching SAOZ observations are EP-TOMS (1995–2004) and OMI-TOMS (2005–2011), whereas for NO<sub>2</sub>, best results are obtained by combining GOME version GDP5 (1996–2003) and SCIAMACHY – IUP (2003–2011), displaying lower noise and seasonality in reference to SAOZ. Both merged data sets are fully consistent with the larger columns of the two species above South America and the seasonality of the differences between the two stations, reported by SAOZ, providing reliable time series for further trend analyses and identification of sources of interannual variability in the future analysis.

## 1 Introduction

The inter-tropical belt is a key region for stratospheric ozone and climate. Indeed, it is the source of all tropospheric short- and long-lived chemical species emitted at the surface, water vapor and sulfate aerosols that are lofted across the tropopause and further transported to higher altitude and latitude by the Brewer–Dobson circulation. The need to understand the impact on the stratospheric composition of the increased emissions of pollutants and greenhouse gases (GHGs), changes in stratospheric circulation, solar activity, quasi-biennial oscillation (QBO) and El Niño events, makes monitoring of the composition of the atmosphere in this region necessary. Hence, it is important to have both ground-based and space-borne observations of trace gases among which ozone and nitrogen dioxide (NO<sub>2</sub>) columns have been measured during the last 20 years. But although total ozone and NO<sub>2</sub> satellite observations by Earth Probe (EP-TOMS), Global Ozone Monitoring Experiment (GOME), followed by Scanning Imaging Absorption Spectrometer for Atmospheric Chartography (SCIAMACHY) and Ozone Monitoring Instrument (OMI), have been thoroughly validated at mid-latitude by comparison with ground-based measurements (e.g. PETERS et al., 2006; BALIS et al., 2007; LAMBERT et al., 1998; CELARIER et al., 2008; IONOV et al., 2008; HENDRICK et al., 2011), with the exception of the last mentioned papers, the validation hardly applies to the tropics. The reason for that

is the limited number of long series of ground-based ozone and NO<sub>2</sub> measurements available at this latitude. Because of the differences in the performances of the satellite retrieval procedures in tropical meteorological conditions such as frequent high altitude cirrus clouds and thunderstorm anvils, their data require validation, corrections and normalization between them before carrying out reliable trend analyses.

The goal of this study is the evaluation of the performance of those total ozone and NO<sub>2</sub> satellite measurements in the tropics, for identifying the best data available for building long series of merged satellite composite series for further trend analyses. The evaluation is performed by a comparison with the long series of ground-based NDACC (Network for Detection of Atmospheric Composition Changes) measurements of well-calibrated and maintained instruments. The data used here are those of two O<sub>3</sub> and NO<sub>2</sub> measuring SAOZ (Système d'Analyse par Observation Zénithale)/NDACC UV-visible spectrometers (Pommereau and Goutail, 1988) deployed in the southern tropics, in the continental region of Bauru (22° S, 49° W) in S-E Brazil in 1995, located in the cloudy South Atlantic convergence zone (SACZ) and on Reunion Island (21° S, 55° E) in the SW Indian Ocean, a clearer oceanic area, since 1993.

The scope of this paper is to look at the continuity of several satellite data sets in the tropics with respect to SAOZ measurements considering their respective drift and seasonal and interannual variations in order to select 'homogenized satellite data' and build long term series over the two stations. The ozone satellite data retrievals available in coincidence with the SAOZ measurements are those of the NASA EP-TOMS V8 (McPeters et al., 1998) between 1996 and 2005, the GOME-ERS2 (European Remote Sensing satellite number 2) (Burrows et al., 1999a) ESA Data Processor version 5 (GDP5) in the 1995–2003 period, the SCIAMACHY-ENVISAT (ENVironment SATellite) (Bovensmann et al., 1999) ESA operational off-line processor version 3 in the 2002–2012 period and the NASA OMI-TOMS (Barthia et al., 2002) and OMI-DOAS (Differential Optical Absorption Spectroscopy) products (Veefkind et al., 2006) from 2004 until present. For NO<sub>2</sub> the data used are those of the GOME and SCIAMACHY Institute of Environmental Physics (IUP) V1 (for the first; Richter et al., 2005) and V2 (for the latter; Richter et al., 2004) retrieval and those of the GOME and SCIAMACHY ESA version GDP5 (for the first, Spurr et al., 2012) and version SGP5 (for the latter, Lichtenberg et al., 2010), and the OMI-DOAS NASA v3 products (Boersma et al., 2002).

This paper is organized as follows: a brief description of the SAOZ and satellite instruments and data used in the analyses is given in Sect. 2. Section 3 provides an analysis of ozone seasonal and interannual variability and difference between the two stations as seen by SAOZ, to which the satellite data are compared, followed by the building of an optimum merged satellite data series. The same analysis is

performed for NO<sub>2</sub> in Sect. 4 and the findings are summarized in Sect. 5.

## 2 Observational data

The data used in this study are the ozone and NO<sub>2</sub> columns from the ground-based SAOZ/NDACC instruments at the two tropical stations of Bauru and Reunion Island and collocated EP-TOMS, GOME, SCIAMACHY and OMI satellite data. Increased scatter and offsets between SAOZ and satellite are expected in case of significant column geographical gradients or large tropospheric contributions. For limiting their impact, Lambert et al. (2012) suggested to use satellite footprints overlapping the SAOZ air mass (a method called optical path matching technique) instead of direct overpass data. The advantage of applying this method for reducing the noise in the differences between data sets is well established in polar and mid-latitude regions where horizontal gradients due to dynamical barriers and vortex intrusions are frequent. However, applying such correction appears unnecessary in the tropics for three reasons (cf. Appendix A): (i) the small satellite overpass frequency which severely reduces the number of collocations, (ii) the very limited O<sub>3</sub> and NO<sub>2</sub> stratospheric total columns horizontal gradients (for example, SAOZ sunrise and sunset columns looking alternatively east and west do not show any significant mean differences), and (iii) the small contribution of surface layer pollution to the total columns outside urban areas. Biases between SAOZ and satellites in the tropics can come only from the retrieval procedure and/or from tropospheric column contributions. Satellite overpass data are thus fully convenient at this latitude. The characteristics of the data used in the following tropical studies are briefly described in the following.

### 2.1 Ground-Based SAOZ UV-visible total NO<sub>2</sub> and O<sub>3</sub> columns

SAOZ is a zenith sky looking UV-Vis spectrometer developed by Pommereau and Goutail (1988) for monitoring the long-term evolution of O<sub>3</sub> and NO<sub>2</sub> total columns which was deployed progressively at a number of stations at all latitudes within the NDACC network, among them Bauru (22° S, 49° W) in southeast Brazil in 1995 and Reunion Island (21° S, 55° E) in the southwest Indian Ocean in 1993 (<http://saoz.obs.uvsq.fr/>). The zenith sky measurements, performed twice a day at sunrise and sunset between 86 and 91° solar zenith angle (SZA) in the visible Chappuis bands, between 450 and 550 nm for O<sub>3</sub> and 410–530 nm for NO<sub>2</sub> with a spectral resolution of 0.8 nm, are analyzed by the DOAS (differential optical absorption spectroscopy) technique (Platt, 1994). At these large SZA, where the scattering altitude of sunlight is between 12 and 15 km in the visible, the measurements are not sensitive to clouds at lower levels, except in the presence of very thick clouds like thunderstorms

or rain showers, where multiple scattering can enhance the tropospheric ozone and NO<sub>2</sub> slant columns. Such events are identified by looking at tropospheric water vapor and oxygen dimer (O<sub>4</sub>) column enhancements and a filter is applied on the SAOZ to reject O<sub>3</sub> and NO<sub>2</sub> measurements in the presence of those events.

The ozone data available are those of the version 2 retrieval algorithms applying the recommendations of the NDACC UV-VIS working group described by Hendrick et al. (2011). The largest change compared to the previous SAOZ version 1 retrieval is the use of a daily air mass factors (AMFs) calculated from the TOMS V8 ozone profile climatology (McPeters et al., 2007) for converting slant into vertical columns, instead of a yearly mean profile used in the previous version 1. The random error estimated by Hendrick et al., is 4.7 % and the total accuracy ~ 5.9 %.

For NO<sub>2</sub>, a yearly mean profile is used built from HALOE (Halogen Occultation Experiment) solar occultation measurements above 20 km, complemented for the lower stratosphere and upper troposphere by SAOZ-balloon profiles measured in Bauru (details of the retrieval can be found in Ionov et al., 2008). However, the use of a yearly mean instead of a daily profile has little impact on the total NO<sub>2</sub> column variations in the tropics since their seasonal change is less than 5 %. The precision of the NO<sub>2</sub> column is about 11 % and the total accuracy ~ 21 % (Ionov et al., 2008). The SAOZ instrument has been qualified by NDACC for ozone and NO<sub>2</sub> measurements during several international inter-comparison campaigns (Vaughan et al., 1997; Vandaele et al., 2005). One of the advantages of the SAOZ technique, particularly useful for long series of measurements and comparing those obtained at two independent stations, is the calibration provided by the absorption cross-sections (the same for the full series of data) used in the DOAS analyses and not requiring regular calibrations for correcting possible shifts like for the other ground-based UV spectrophotometers. The two other advantages of the technique for comparison with satellite observations are the absence of temperature dependence of the ozone absorption cross-sections in the visible Chappuis bands in contrast to the UV, and the constant 86–91° SZA of observations not varying with the season as is the case in satellite observations (Hendrick et al., 2011).

## 2.2 EP-TOMS

EP-TOMS, is a six-wavelength-nadir-viewing instrument on the helio-synchronous Earth Probe (EP) satellite, crossing the equator at 11:00 LT which operated between July 1996 and the end of 2005 (McPeters et al., 1998). The data used here are those of the version 8 retrieval algorithm available on (<ftp://jwocky.gsfc.nasa.gov/pub/eptoms/data/overpass/>). The ozone measurements are based on a differential pair method at 317.5 and 331.2 nm for a SZA smaller than 70° always available in the tropics (Wellemeyer et al., 2004). The estimated accuracy is about 3 to 5 %. Since 2000, EP-TOMS

experienced instrumental problems introducing a 3 % bias in total ozone (Bramstedt et al., 2003). For the version 8, an empirical correction was applied by NASA to overcome this bias (McPeters et al., 2007).

## 2.3 GOME

The GOME instrument (Global Ozone Monitoring Experiment) was launched on 21 April 1995 aboard the ESA ERS-2 satellite, into a 795 km altitude sun-synchronous orbit of 98.5° inclination. GOME is a nadir-viewing spectrometer, which observes solar radiation reflected or scattered by the atmosphere and the land surface in the UV-visible spectral range (240–790 nm) with a spatial resolution of 320 × 40 km (Burrows et al., 1999a). The satellite passes over the equator during the descending part of the orbit at 10:30 LT. The instrument was designed to measure trace gases in the troposphere and the stratosphere, including ozone, and was the first space instrument to measure NO<sub>2</sub> total columns. Global coverage is achieved in 3 days. The ozone data used here are the GOME ESA version GDP 5.0 level 2 products (ftp server: <http://ftp.eoa-dp.eo.esa.int>) retrieved between 325 and 335 nm with an analysis based on the GOME Direct Fitting algorithm (GODFIT algorithm) created by the Belgian Institute for Space Aeronomy (BIRA), the German Aerospace Centre (DLR) and RT Solutions Inc. (detail of the algorithm can be found in Spurr et al., 2012). From this version, the estimated accuracy is about 3.6–4.3 % for SZA lower than 80° and about 6.4–7.2 % for SZA between 80 and 90° (Loyola et al., 2012).

For NO<sub>2</sub>, two retrievals are used: (i) the version 1 of the Institute of Environmental Physics (IUP) of the University of Bremen GOME (Richter et al., 2005) and (ii) the ESA GOME Data Processor GDP version 5 (same algorithm as version GDP4 (Loyola et al., 2012)). Both are using the same cross-sections (Burrows et al., 1999b) at 221 K and the DOAS spectral analysis method between 425–450 nm. The Data Processor GDP version 5 retrieval is based on the GODFIT-DOAS (GDOAS) algorithm created by the Belgian Institute for Space Aeronomy (BIRA-IASB) (Van Roozendael et al., 2006). The difference between the two versions comes from the different air mass factors (AMFs) used and the correction applied for the diffuser offset. Both versions provide total column based on a stratospheric AMF, not including tropospheric contributions. In the IUP product, the AMF are calculated with the radiative transfer model SCI-ATRAN (Rozanov et al., 2005) using a US standard atmosphere profile with the troposphere set to 0 (Richter et al., 2005). In the ESA product, the columns are derived from AMFs calculated with the multiple scattering radiative transfer model LIDORT (linearized discrete ordinate radiative transfer) (Spurr et al., 2001) using a NO<sub>2</sub> profile climatology (Lambert and Balis, 2004). To compensate the effect of spectral artifacts in GOME solar spectra due the varying diffuser illumination angles, the IUP retrieval applies a

normalization on each slant column using a slant column measured over the clean Pacific, assuming in this area a vertical column of  $2 \times 10^{15}$  molec cm<sup>-2</sup>, independent of the season. The resulting columns are assumed to be a good estimation of stratospheric columns in clean areas, but they may be larger than the stratospheric column in polluted areas (Richter et al., 2005). The accuracy is estimated at 5–10%. The data used here are available on [http://www.doas-bremen.de/gome\\_no2\\_data\\_quilt.htm](http://www.doas-bremen.de/gome_no2_data_quilt.htm). On the GDP5 product, an optimal calibration is applied on the post-processed data whose details can be found in Lambert and Balis (2004). The accuracy is estimated between 5 and 10% in unpolluted areas. The data used here are available at the following address: [http://wdc.dlr.de/data\\_products/TRACEGASES/](http://wdc.dlr.de/data_products/TRACEGASES/).

Following the failure of the last on-board recorder in 2002, the ERS-2 spatial coverage was reduced and no data were available in the southern tropics after this date.

## 2.4 SCIAMACHY

The SCIAMACHY (Scanning Imaging Absorption Spectrometer for Atmospheric Chartography) instrument was launched on March 2002 on the ENVISAT platform. The satellite crosses the equator at 10:00 LT on a sun-synchronous orbit at 800 km of 98.5° inclination. SCIAMACHY is a spectrometer that measures solar radiation scattered by the atmosphere at limb and nadir in the spectral UV-visible range (240–790 nm) with a spectral resolution of 0.2 to 1.5 nm and a spatial resolution of  $30 \times 60$  km<sup>2</sup> (Bovensmann et al., 1999). The high spectral resolution and the use of a wide range of wavelengths allow the detection of several trace gases. Because of the alternate nadir and limb observations, its global coverage is of 6 days, a factor of 2 lower than that of GOME. The ozone data used in this study are those of the ESA operational off-line processor version 3.01 ([http://wdc.dlr.de/data\\_products/TRACEGASES/](http://wdc.dlr.de/data_products/TRACEGASES/)). This product has been developed based on GOME GDP4.0 (Bracher et al., 2005). The estimated accuracy is about 5% for SZA lower than 60°.

As for GOME, two NO<sub>2</sub> retrievals are used in this study, one from the Institute for Environmental Physics (IUP) of the University of Bremen (Richter et al., 2004) version 2 and the other one from the ESA off-line Processor SGP version 5.02 (Lichtenberg et al., 2010). Both versions are using the same cross-sections (Bogumil et al., 2003) at 243 K and a DOAS spectral analysis method between 425–450 nm. The data processor version 5.02, for the trace-gas slant column retrieval, is based on the SDOAS algorithm created by BIRA-IASB. THE SDOAS algorithm is the adaptation of GDOAS to the SCIAMACHY instrument (hereafter named SDOAS to easily distinguish it from the GOME version). Both products use the same AMF as described in the section on GOME data. The only exception is that for SGP HALOE profiles are used instead of a climatology (Lambert et al., 2000).

The estimated accuracy for the IUP version is about 5 to 10% (Richter et al., 2004) and the data can be found at [http://www.iup.uni-bremen.de/doas/scia\\_no2\\_data\\_acve.htm](http://www.iup.uni-bremen.de/doas/scia_no2_data_acve.htm).

The estimated accuracy of the SGP version ranges from 5 to 20% at polar latitudes and in the Northern Hemisphere. The NO<sub>2</sub> columns are low biased by about  $5 \times 10^{14}$  molec cm<sup>-2</sup> at low and middle latitudes of the Southern Hemisphere. This low bias exhibits a seasonal cycle (larger in summer) and a latitudinal dependence. The NO<sub>2</sub> columns are affected by larger errors over polluted areas (large underestimation of total column) and in the South Atlantic Anomaly. (link: [https://earth.esa.int/handbooks/availability/disclaimers/SCI\\_OL\\_2P\\_README.pdf](https://earth.esa.int/handbooks/availability/disclaimers/SCI_OL_2P_README.pdf)) The data can be ordered via the ESA EO Principal Investigator Portal.

## 2.5 OMI

The OMI (Ozone Monitoring Instrument) was launched on 15 July 2004 aboard the Earth Observation satellite Aura sun-synchronous platform at 705 km of 98.2° inclination (Levelt et al., 2006). OMI is a nadir-viewing UV/Visible spectrometer with a spectral resolution of about 0.63 nm for the visible channel (349–504 nm) and about 0.42 nm for the UV channel (307–383 nm). It measures the solar light scattered by the atmosphere in the 270–500 nm wavelength range with a spatial resolution at nadir of  $13 \text{ km} \times 24 \text{ km}^2$ . The satellite crosses the equator during the ascending part of the orbit at 13:42 LT. In this study, two algorithms are used for total ozone. The first, called OMI-TOMS, is identical to that used for EP-TOMS V8 (Bucharth et al., 2008) providing total ozone measurements with a relative uncertainty of 2% at SZA lower than 70° and increasing to 5% at 85° (Barthia et al., 2002). The second, called OMI-DOAS, developed by KNMI (Koninklijk Nederlands Meteorologisch Instituut) is based on the DOAS method with a relative accuracy of 3% on cloudy days and 2% at clear sky (Veeffkind et al., 2006). The data of the two versions are available from <http://avdc.gsfc.nasa.gov/>.

For NO<sub>2</sub>, the OMI data version 3 used here is that developed by NASA, using the cross-sections of Vandaele et al. (1998) at 220 K and the DOAS technique in the wavelength interval 405–465 nm (Boersma et al., 2002). The vertical columns are calculated with a stratospheric AMF, which depends on the viewing geometry, the surface albedo and the shape of the NO<sub>2</sub> vertical profile. As described in Ionov et al. (2008), for each location, the algorithm uses a single mean unpolluted profile derived from a stratospheric model and a geographically gridded set of annual mean polluted profiles provided by a tropospheric model. An initial estimate of the NO<sub>2</sub> vertical column is obtained by dividing the slant column by an unpolluted AMF, geographically gridded using the data acquired within  $\pm 12$  h from the target orbit. Areas shown by the model to contain climatologically high tropospheric NO<sub>2</sub> amounts are then masked, and the remaining regions are smoothed in latitude bands to construct

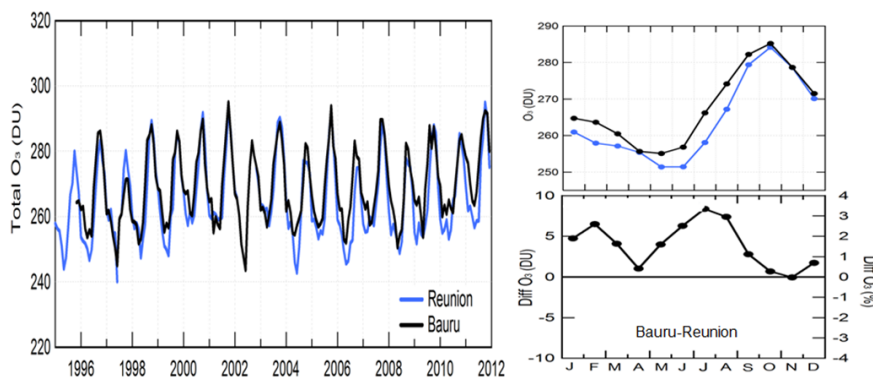


**Figure 1.** left: Monthly mean time series of SAOZ total O<sub>3</sub> in Bauru (black) and Reunion (blue). Top right, seasonal variation in Bauru and Reunion. Bottom right: difference between the two stations.

a global stratospheric field. Where the initial vertical column exceeds the estimated stratospheric NO<sub>2</sub>, the presence of tropospheric NO<sub>2</sub> is inferred and the vertical column is recalculated using an AMF computed from an assumed tropospheric NO<sub>2</sub> profile (Bucsela et al., 2006). The estimated accuracy of the NO<sub>2</sub> vertical column in clear sky and unpolluted conditions is 5 % ( $0.2 \times 10^{15}$  molecules cm<sup>-2</sup>) and 20 % ( $0.8 \times 10^{15}$  molecules cm<sup>-2</sup>) in polluted cases. In the presence of pollution and clouds, the error can reach 50 % (Celarier et al., 2008; Boersma et al., 2002). The data are available at <http://avdc.gsfc.nasa.gov/>.

### 3 SAOZ and satellites total ozone

Assuming that SAOZ data is the ground-truth reference, the first step before the comparison with satellite is the characterization and the understanding of the origin of seasonal and interannual variations seen by SAOZ as well as of the differences reported between the two stations. Note that since the eruption of the Pinatubo volcano in 1991 resulted in the perturbation of both ground-based zenith sky and satellite nadir measurements until 1993–1994, the data before 1995 will be ignored in the following.

#### 3.1 SAOZ observations

The SAOZ monthly mean O<sub>3</sub> columns in Bauru and Reunion since 1995, the average seasonal variations over the two stations and the difference between them are displayed in Fig. 1. In both stations the long-term mean column is of about 270 DU with a seasonal cycle of 30–40 DU amplitude with maximum in spring. The interannual variations are also very similar, displaying a biennial cycle of about 10 DU amplitude linked to the QBO (quasi biennial oscillation). In the long term, both stations are showing a slight increase of 15 DU between 1995–2002, followed by stabilization between 2003–2007 and an increase by 20 DU (more pronounced at Bauru) after 2008. The difference between the

two stations shows larger ozone over Bauru than Reunion during the austral summer ( $\sim 2\%$ , about 5 DU in January–March) and during the winter ( $\sim 3\%$  about 6–7 DU in May–August). The larger summer ozone columns over Bauru during the thunderstorm season are consistent with the known photochemical ozone production in the upper troposphere by lightning NO<sub>x</sub> (LNO<sub>x</sub>) and entrainment of O<sub>3</sub> rich air masses from the upper troposphere–lower stratosphere region as shown by Rivière et al. (2006) and Huntrieser et al. (2008). The larger total ozone in winter over Bauru is of different nature. It originates from the more northern location of the high tropical jet in the winter over South America than over the Indian Ocean as shown by the equivalent latitude difference at 450 and 475 K potential temperature levels (Fig. 2), derived from the potential vorticity (PV) of the high-resolution contour advection model MIMOSA (Modélisation Isentrope du transport Méso-échelle de l’Ozone Stratosphérique par Advection, Hauchecorne et al., 2002), resulting in a stronger influence of mid-latitude ozone over Bauru. In summary, the ozone seasonal and interannual variations are very similar above the two stations. The only differences between them are the larger upper tropospheric ozone over the continent during the thunderstorm season, and the larger influence of mid-latitude ozone in the lower stratosphere in winter.

#### 3.2 Comparison between satellites and SAOZ

The monthly mean GOME-GDP5, EP-TOMS, SCIAMACHY-OL3, OMI-TOMS, OMI-DOAS total ozone, and the SAOZ sunrise–sunset average are shown in Fig. 3, and the seasonal variation of the differences satellite–SAOZ in Fig. 4 for Bauru and Figs. 5 and 6 for Reunion. Mean biases and standard deviations with SAOZ are summarized in Table 1. Systematic biases are observed between satellites and SAOZ. With the exception of the beginning of GOME in 1995 and EP-TOMS in late 2002 (immediately after the correction for the instrumental problems), the satellites are lower on average by 5.2 DU ( $-1.9\%$ ) in Bauru and closer by 0.3 DU ( $0.1\%$ ) in Reunion.

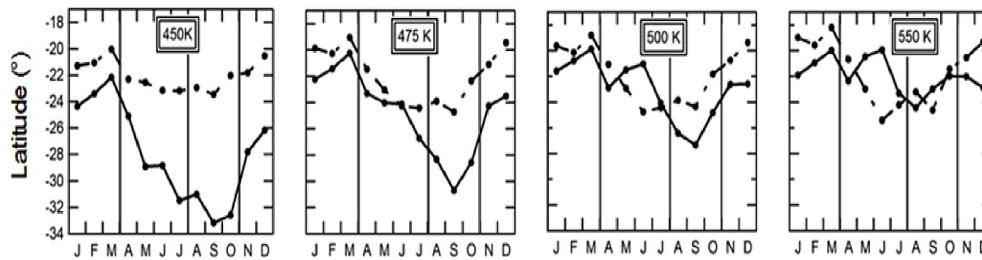


**Figure 2.** Equivalent latitude seasonal variation above Bauru (solid line) and Reunion (dashed) at 450, 475, 500 and 550 K potential temperature levels. The stratosphere over Bauru, north of the tropical jet in the winter, is much more influenced by the mid-latitudes.

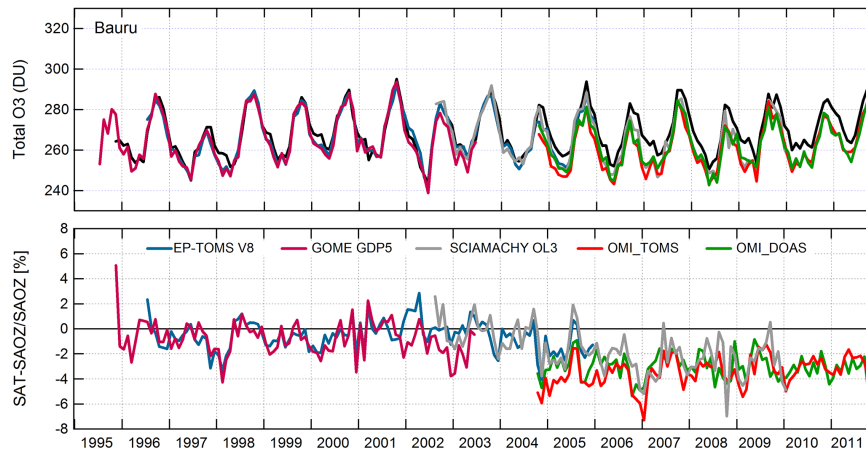


**Figure 3.** Total ozone over Bauru. Top: monthly mean column GOME GDP5 (pink), EP-TOMS (blue), SCIAMACHY OL3 (grey), OMI-TOMS (red), OMI-DOAS (green) and SAOZ sunrise–sunset average (black); Bottom: differences with SAOZ.

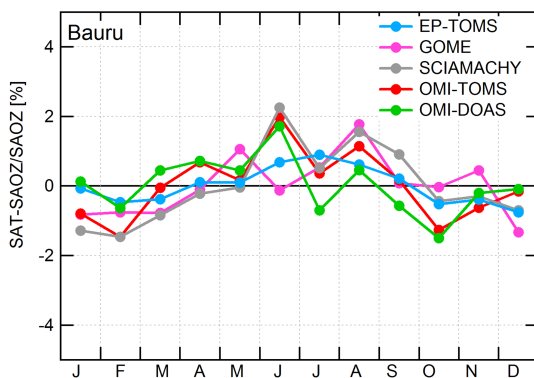


**Figure 4.** Relative difference of the seasonal ozone cycle between satellite and ground based observations at Bauru. GOME GDP5 (pink), EP-TOMS (blue), SCIAMACHY OL3 (grey), OMI-TOMS (red), OMI-DOAS (green).

For Bauru, EP-TOMS columns show the smallest differences with the SAOZ measurements (mean bias of  $-0.59\%$ ). GOME columns are lower than those from SAOZ ( $-0.7\%$ ) and present the same variations as EP-TOMS until 2001 where an increase of the difference is observed. The two versions of OMI exhibit relatively the same variations and

on average the same different amounts of O<sub>3</sub> ( $-3.4\%$  for OMI TOMS and  $-3.1\%$  for OMI DOAS) relative to SAOZ columns. The difference with SCIAMACHY is similar to EP-TOMS until 2005 then increases and becomes as large as that for the OMI versions.

Because each satellite presents different long-term variations, the evaluations of satellite data drifts with respect to the SAOZ have been calculated with a linear regression on the relative differences. From this analysis, only SCIAMACHY exhibits a significant drift with respect to the SAOZ ( $0.3\% \text{ yr}^{-1}$  for SCIAMACHY compared to less than  $0.04\% \text{ yr}^{-1}$  for the other). Finally, a seasonal variation of the difference between each satellite and SAOZ is observed. In order to highlight those biases, Fig. 4 presents the relative difference between satellite and SAOZ seasonal cycle. It should be noted that the data have been normalized in order to make variations comparable. In this figure, all satellite data present a seasonal variation of the difference with a minimum during the austral summer (mean difference of  $1\%$ ) and a maximum during the austral winter, except for OMI-DOAS. EP-TOMS presents the smallest bias with a minimum  $-0.7\%$  during austral summer and a maximum of  $0.7\%$  during austral winter. SCIAMACHY and OMI-TOMS

**Table 1.** Mean biases and standard deviation in DU (%) between satellites and SAOZ total ozone.

Satellite	Bauru	Reunion
EP-TOMS	$-1.58 \pm 3.1$ (−0.59)	$2.80 \pm 3.6$ (1.04)
GOME–GDP5	$-2.05 \pm 3.6$ (−0.77)	$0.81 \pm 3.8$ (0.29)
SCIAMACHY–OL3	$-4.93 \pm 4.7$ (−1.7)	$-0.73 \pm 2.9$ (−0.24)
OMI–DOAS	$-8.13 \pm 2.9$ (−3.1)	$-2.67 \pm 2.5$ (−1.02)
OMI–TOMS	$-9.47 \pm 3.2$ (−3.4)	$1.31 \pm 3.4$ (0.47)
AVERAGE	$-5.2$ (−1.9)	$0.3$ (0.1)

presents on average the same variations. Finally, OMI-DOAS observes less O<sub>3</sub> (−1.5 %) from July to October.

For Reunion (Fig. 5), no satellite presents a significant mean bias. GOME and EP-TOMS exhibit similar variations, with a larger seasonal variation (minimum in austral winter). EP-TOMS columns are higher than those of SAOZ (1.04 %) with large variations. The two versions of OMI present similar variations, nevertheless OMI-TOMS columns show larger values than the SAOZ (0.47 %) and present a shift of  $\approx 1.4$  % with OMI-DOAS. SCIAMACHY variations are similar to EP-TOMS and OMI-TOMS. Regarding the evolution of satellite measurements with respect to the SAOZ, all satellites present non-significant drifts (0.2 % yr<sup>−1</sup> in average). Finally, as at Bauru, a seasonal variation of the difference between each satellite and SAOZ is observed; those biases are highlighted in Fig. 6 representing the relative difference between the seasonal cycle in satellite and SAOZ data. From January to March, SAOZ columns are systematically higher than all the satellites with a bias of on average 1 %. OMI-TOMS presents the maximum bias during his period (−2 %) and EP-TOMS the smallest (−0.7 %). From June to December, the difference between satellites and SAOZ is positive and relatively constant.

Mean biases between satellites and SAOZ ozone and between satellites themselves may originate from errors in the absorption cross-sections, tropospheric ozone, and instrumental drift. But as shown by the small ( $< \pm 1$  %) biases between all series of data in Reunion, the impact of these, at least under clear sky conditions, is limited. On the retrieval aspect, the best indicator is the seasonality of the difference. This may result from cross-section temperature and satellite SZA dependencies as well as cloud masks. As shown by Hendrick et al. (2011) the largest temperature dependence between satellites and SAOZ is observed with TOMS (0.21 % °C<sup>−1</sup>), half with OMI-TOMS and smaller with all others, whereas the largest SZA dependence is observed with the SCIAMACHY-TOSOMI (SCIAMACHY total ozone retrieval algorithm) retrieval not used here. However, because of the limited seasonality of stratospheric temperature and the small SZA at satellite overpasses, the impact of these dependencies is limited ( $< +1$  %) in the tropics. As shown by the bias drop in the January–March period in Reunion (Fig. 6) and in the October–March period in Bauru (Fig. 4)

and the larger noise there, the most important contributor to uncertainties may come from the cloud cover.

Indeed, the ozone minimum period coincides exactly with that of the high clouds presence: thick thunderstorms from September to February in Brazil and hurricane season from January to March in Reunion. Since there is no significant tropospheric ozone seasonal variation matching these changes, the most likely explanation for these variations is the partial masking of tropospheric ozone replaced in the retrievals by a climatology of ozone below the cloud top, which seem to underestimate the ozone content. The “cloud correction” is highly variable from one satellite retrieval procedure to another (more details of the “cloud correction” between DOAS and GODFIT procedure can be found in Van Roozendael et al., 2012).

From all satellite-SAOZ differences in Bauru and Reunion displayed in this section, the best satellite combination for covering the full SAOZ 1995–2011 period are EP-TOMS (1995–2004) and OMI-TOMS (2005–2011) showing smallest instruments shifts and seasonality, but requiring a correction offset for systematic biases with SAOZ.

### 3.3 Merged satellite total ozone series

Following these conclusions, a merged satellite composite series, displayed in Fig. 7, has been constructed with the EP-TOMS and OMI-TOMS data after normalization by addition of their respective biases with SAOZ shown in Table 1.

The merged series show high correlation with SAOZ of 0.96 in Bauru and 0.97 in Reunion, although of slightly larger slope (0.95 instead of 0.87) and larger intercept (32 DU instead of 12 DU) over Reunion compared to Bauru. The seasonal variations of the difference between the two stations seen by the merged satellite and SAOZ series are shown in Fig. 8. The satellite series confirms the larger ozone in Bauru seen by SAOZ in summer (January–March) and winter (June–August), but differs in spring (October–November) when the satellites are reporting a 5.7 DU larger column over Reunion. As explained in Sect. 3.1, the 5 DU larger column over Bauru seen by both data sets during the summer convective season is due to the photochemical ozone production in the upper troposphere, where both nadir satellite and ground-based zenith sky measurements are sensitive. The

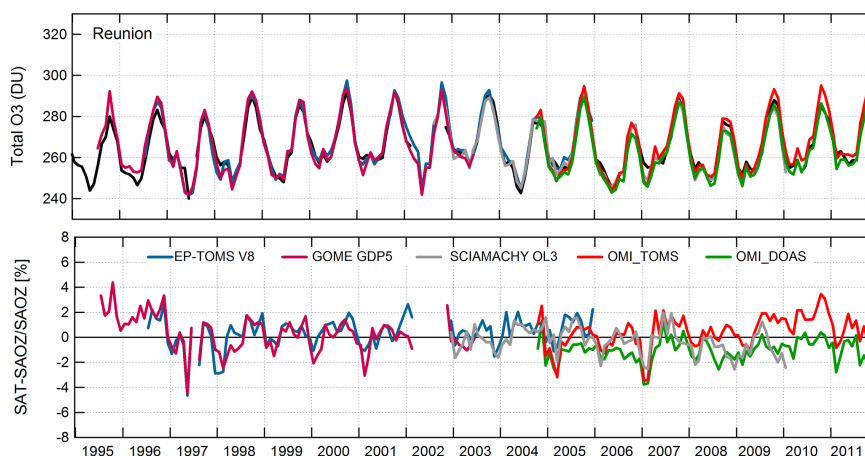


Figure 5. Same as Fig. 3 but for Reunion.

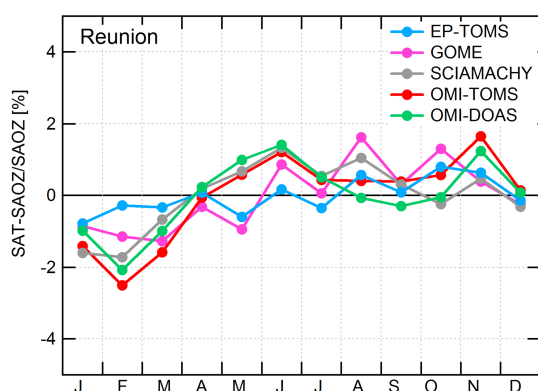


Figure 6. Same as Fig. 4 but for Reunion.

same applies to the 10 DU maximum in the winter attributed to the ozone longitudinal variation in the lower stratosphere. The only difference between the two data sets is the largest column (5 DU) in Reunion in the October–November period. The explanation of this difference is the advection of a biomass-burning plume over the Indian Ocean from Africa, resulting in an increase of ozone concentration in the middle troposphere over Reunion between 5–12 km (Randriambelo et al., 2000). The smaller sensitivity of SAOZ compared to the one of the satellites when considering this event is due to the low altitude of the ozone-rich layer to which ground-based zenith sky twilight measurements are less sensitive than the nadir-viewing satellites.

In conclusion, with the exception of a mid-tropospheric ozone increase over Reunion during the African biomass-burning season to which SAOZ is less sensitive, the EP-TOMS (1995–2004) and OMI-TOMS (2005–2011) satellite merged ozone series fully agrees with the SAOZ series in the Southern tropics. Both are showing larger ozone columns over the South American continent compared to the southwest Indian Ocean.

## 4 SAOZ and Satellite NO<sub>2</sub> columns

A similar analysis for NO<sub>2</sub> has been carried out on SAOZ and satellite NO<sub>2</sub> measurements with the difficulty, compared to the previous measurements, of a photochemical diurnal variation of the species requiring correction prior to comparison and of a larger contribution of tropospheric content above polluted areas.

### 4.1 SAOZ observations

The SAOZ sunrise and sunset monthly mean columns in Bauru and Reunion are displayed in Fig. 9 on the left, and the seasonal variation at the two stations and the difference between them on the right. On average, the NO<sub>2</sub> column is larger by  $0.7 \times 10^{15} \text{ mol cm}^{-2}$  in Bauru. The seasonal and interannual variations are very similar at both stations, displaying a maximum in 1997–1998 in phase with the largest El-Niño event during the period and a quasi-biennial cycle of  $0.5 \times 10^{15} \text{ mol cm}^{-2}$  amplitude with a maximum during the west phase of the quasi-biennial oscillation (QBO). At both stations, the seasonal variation exhibits a spring maximum, but of larger amplitude ( $0.5 \times 10^{15} \text{ mol cm}^{-2}$ ) which is delayed by 1 month in Bauru. The difference between the two stations (Fig. 9, bottom right) also shows a seasonal cycle with a 38 % larger column over Bauru in the summer in the November–March period, a little larger at sunset, and a smaller increase of 20–25 % in the July–August period, larger at sunrise.

The factors contributing to the differences between the two stations are as follows: (i) the longitudinal variation in the lower stratosphere in winter, like that shown for ozone and, (ii) the tropospheric NO<sub>2</sub> column. As for ozone, the contribution to the total column is important.

The increase of tropospheric NO<sub>2</sub> in the winter–spring period (late August, seen Fig. 9 on the right) is related to sugar cane fires, as reported for example by the GOME NO<sub>2</sub>

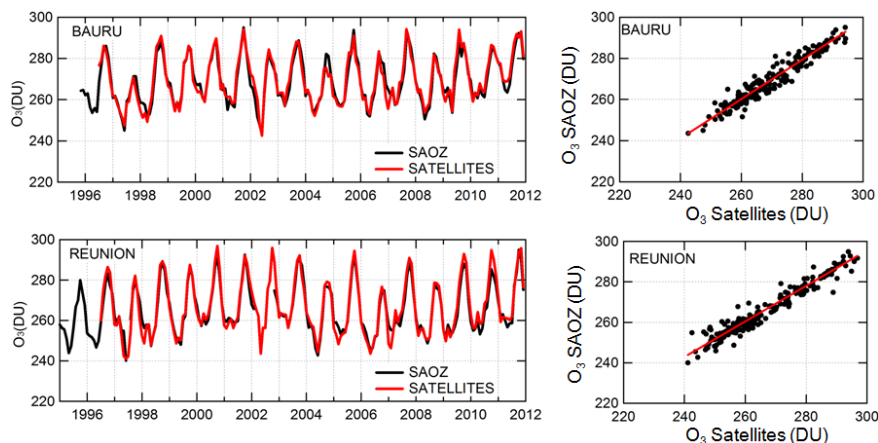


**Figure 7.** Left: Time series of SAOZ (black) and merged satellites (red) total O<sub>3</sub> column (DU) in Bauru (top) and Reunion (bottom). Right: Correlation between SAOZ and merged satellites ( $r^2 = 0.96$  in Bauru and  $r^2 = 0.97$  in Reunion).

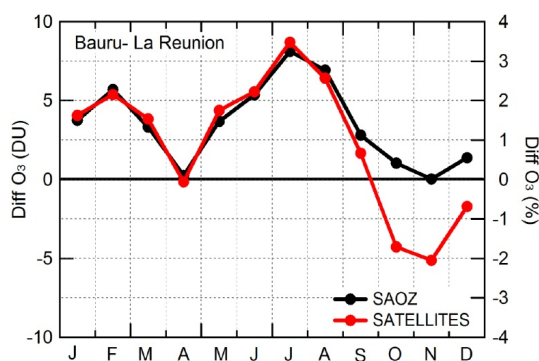


**Figure 8.** Seasonal cycle of the ozone difference between Bauru and Reunion for SAOZ (black) and merged satellite composite (red).

observations (Richter and Burrows, 2002). The larger NO<sub>2</sub> concentration in the lower stratosphere in winter, due to the higher equivalent latitude of Bauru (Fig. 2), is confirmed by the difference between HALOE NO<sub>2</sub> sunrise mean profiles (Russel et al., 1993) within a 200 km radius above the two stations in the August–October period shown in Fig. 10. To get the maximum profiles, the satellite grid observation has been expanded to 200 km radius around the station (Bauru:  $22^\circ \pm 3^\circ$  S,  $50^\circ \pm 15^\circ$  W, Reunion:  $20 \pm 3^\circ$  S,  $50 \pm 15^\circ$  E). Despite this extension, only 100 profiles were used at Bauru and 110 at Reunion. Because of the extension of the grid and the time of satellite measurement (between 7 and 9 a.m.), all profiles had to be standardized from a reference profile calculated using a photochemical box model derived from the 3-D off-line chemical transport model SLIMCAT (Denis et al., 2005). As shown in Fig. 10, the NO<sub>2</sub> concentration is larger by  $\sim 0.2 \times 10^9$  molecules  $\text{cm}^{-3}$  in the lower stratosphere above Bauru than above Reunion in winter. Finally, the larger column over South America in austral summer is the result of the lightning NO<sub>x</sub> production between 10–15 km

during the thunderstorm season (Pommereau et al., 2004; Rivière et al., 2006; Huntrieser et al., 2008), as opposed to the Indian Ocean and maritime areas in general where lightning is infrequent (Zipser et al., 2006).

## 4.2 Satellite observations

Figure 11 displays the monthly mean time series of GOME and SCIAMACHY version GDP, SGP and IUP, and OMI-NASA columns at the time of satellite overpass over the equator around 10:00 LT for SCIAMACHY, 10:30 for GOME and 13:00 for OMI. The measurements all show a seasonal cycle with a spring maximum, but of variable amplitude depending on the satellite. In addition they display larger noise in Bauru, suggesting larger NO<sub>2</sub> column variability there, particularly GOME-GDP5 and SCIAMACHY SGP5 measurements. GOME-GDP5 exhibits a larger seasonality than GOME-IUP by  $1.5 \times 10^{15}$  mol  $\text{cm}^{-2}$  in Bauru and  $1.2 \times 10^{15}$  mol  $\text{cm}^{-2}$  in Reunion, larger than both SCIAMACHY versions by  $0.5 \times 10^{15}$  mol  $\text{cm}^{-2}$  in both stations. The latter present similar variability, but the SGP version is noisier. OMI agrees with SCIAMACHY in Bauru, but shows larger columns by  $0.5 \times 10^{15}$  mol  $\text{cm}^{-2}$  in Reunion with less seasonality.

### 4.2.1 Correction for NO<sub>2</sub> diurnal variation

Since NO<sub>2</sub> displays a photochemical diurnal variation and SAOZ and satellite measurements do not coincide in time, a correction is required for comparing their measurements. Figure 12 shows the diurnal variation of the NO<sub>2</sub> column at  $20^\circ$  S in January and June simulated by the SLIMCAT 3-D Chemical Transport Model (Chipperfield, 1999; Denis et al., 2005). The arrows indicate the local time of the satellite overpasses and the full circles that of the weighted average twilight SAOZ measurements between  $86\text{--}91^\circ$  SZA. The simulated satellite columns at the time of

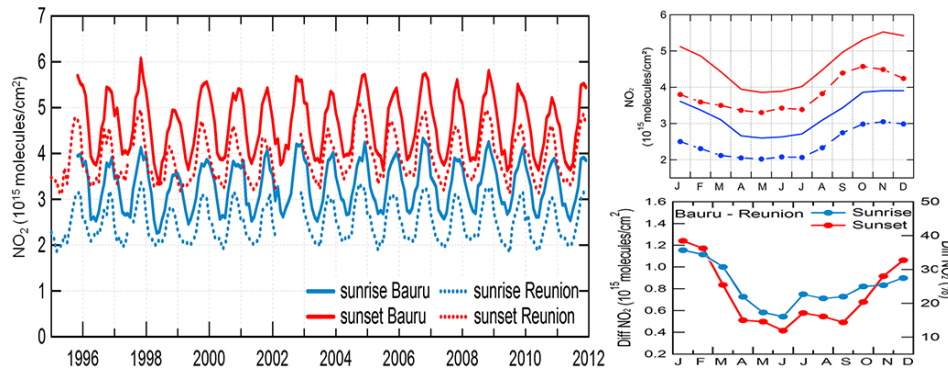


**Figure 9.** Left: monthly mean time series of SAOZ total NO<sub>2</sub> columns at sunrise (blue) and sunset (red) in Bauru (solid lines) and Reunion (dotted). Top right, seasonal variation in Bauru and Reunion. Bottom right: difference between the two stations.

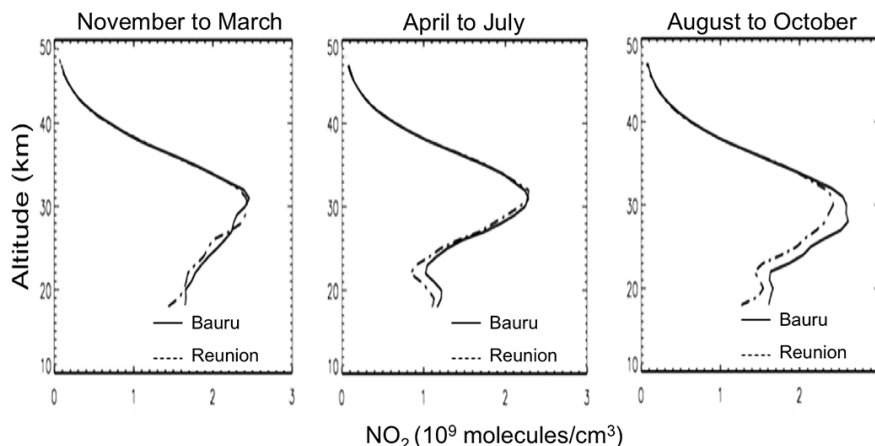


**Figure 10.** HALOE (1995–2005) NO<sub>2</sub> mean profiles over Bauru (solid line) and Reunion (dashed) in the November–March period (left), April–July (middle), and August–October (right).

their overpasses are smaller than those of SAOZ at twilight ( $\sim 0.2 \times 10^{15}$  molecules  $\text{cm}^{-2}$  at sunrise and around  $1.1 \times 10^{15}$  molecules  $\text{cm}^{-2}$  at sunset). Although there is only 30 minutes between GOME and SCIAMACHY and 3 h with OMI, the diurnal variation induces a bias of  $0.05 \times 10^{15}$  molecules  $\text{cm}^{-2}$  between the two first and of  $0.3 \times 10^{15}$  molecules  $\text{cm}^{-2}$  with the last. Moreover, following the seasonal variation, winter columns are greater ( $0.4 \times 10^{15}$  molecules  $\text{cm}^{-2}$ ) than summer ones. Following these various biases observed between satellites and SAOZ, and the exact time when the satellites overpass the station, a diurnal correction is applied to convert all satellite data to SAOZ sunrise time of measurement. The diurnal cycle has been simulated with the above mentioned photochemical box model. In order to correct satellite data, a reference column calculated from the weighted average of SAOZ sunrise measurements between  $86$  and  $91^\circ$  SZA has been defined. The calculation of the diurnal variation of the ratio NO<sub>2</sub> (reference)/NO<sub>2</sub> (model) has been performed for the twelve months of the year. Then, all the satellite measurements have been normalized using this ratio.

### 4.3 Comparison between Satellites and SAOZ

The monthly mean GOME GDP5 and IUP, SCIAMACHY SGP5 and IUP, and OMI satellite data corrected to SAOZ measurement time at sunrise over both stations are shown in Fig. 13, the difference between satellites and SAOZ in Fig. 14, and the seasonal variation of the differences in Fig. 15. Mean biases and standard deviations of the differences with SAOZ are summarized in Table 2.

Systematic and offset biases are observed between the various satellite data versions and SAOZ. Over Bauru, the satellites are lower on average by  $-0.46 \times 10^{15}$  molecules  $\text{cm}^{-2}$  ( $-14.1\%$ ) and closer to SAOZ by  $0.06 \times 10^{15}$  molecules  $\text{cm}^{-2}$  ( $2.6\%$ ) in Reunion. For GOME, the GDP5 retrieval agrees better with SAOZ over the two stations than IUP's, showing smaller bias ( $-6.3\%$  in Bauru and  $0.8\%$  in Reunion) and lesser seasonality (correlation 0.91 instead of 0.65 for IUP over Bauru and 0.95 instead of 0.73 for IUP over Reunion). At both stations, GOME IUP is showing larger seasonality amplitude ( $0.3 \times 10^{15}$  molecules  $\text{cm}^{-2}$ ) compared to SAOZ. The difference between the two GOME

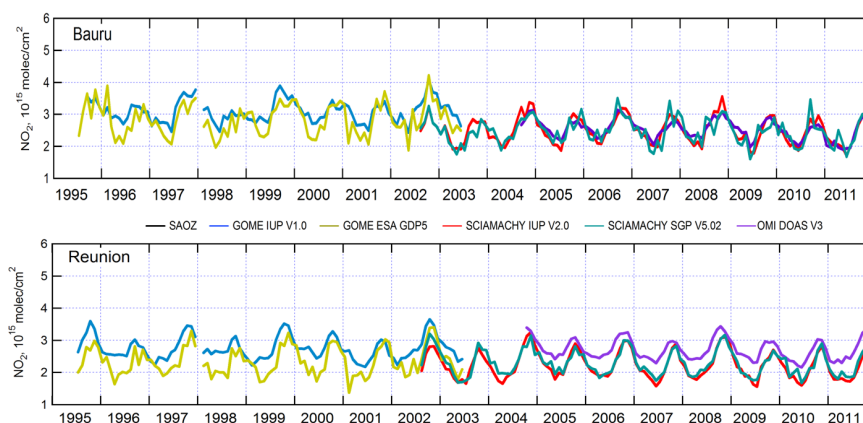


**Figure 11.** Monthly mean NO<sub>2</sub> time series of GOME GDP5 (green), GOME IUP V1 (blue), SCIAMACHY IUP V2 (red), SCIAMACHY SGP V5.02 (dark green), and OMI DOAS V3 (purple) total NO<sub>2</sub> over Bauru (top) and Reunion (bottom).

**Table 2.** Mean biases and standard deviation in  $10^{15}$  molecule  $\text{cm}^{-2}$  (%) between satellites and SAOZ NO<sub>2</sub> columns.

Satellite	Bauru	Reunion
GOME V1.0 IUP	$0.04 \pm 0.5$ (2.6)	$0.44 \pm 0.3$ (19.1)
GOME GDP5 ESA	$-0.21 \pm 0.3$ (-6.3)	$0.02 \pm 0.2$ (-0.8)
SCIAMACHY V2.0 IUP	$-0.63 \pm 0.3$ (-18.8)	$-0.10 \pm 0.1$ (-4.1)
SCIAMACHY SGP5.2 ESA	$-0.62 \pm 0.4$ (-18.9)	$-0.01 \pm 0.2$ (-0.57)
OMI DOAS V3	$-0.9 \pm 0.28$ (-28.9)	$-0.008 \pm 0.2$ (0.28)
AVERAGE	$-0.46$ (-14.1)	$0.06$ (2.6)

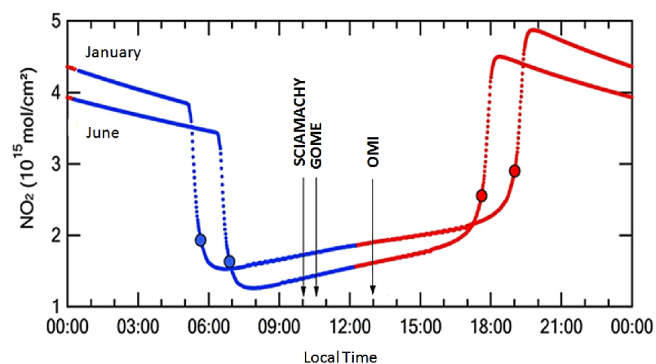


**Figure 12.** Simulated NO<sub>2</sub> column diurnal variation in the tropics in January and July. The markers show the time of sunrise (blue) and sunset (red) SAOZ measurements at 90° SZA and the arrows that of ERS-2 GOME, Envisat SCIAMACHY and Aura OMI overpasses.

retrievals is coming from the different AMF calculation and the correction applied for the diffuser offset (cf. Sect. 2.3), which appears to be less efficient in the IUP data. For SCIAMACHY, both versions display similar seasonality at the two stations and they both agree with SAOZ ( $r^2 = 0.90$  in Bauru and 0.92 in Reunion), the ESA version being a little noisier. In Bauru, they both underestimate the column by 19 %, compared to SAOZ. The IUP version shows less seasonality in

the differences to SAOZ at both stations compared to SGP5 version, which exhibits a maximum of 8 % from March to October and a minimum from November to February at Bauru. The mean bias between GOME and SCIAMACHY in 2003 is less pronounced with the ESA version in Bauru and small in Reunion, compared to IUP. OMI underestimates the columns in Bauru (-29 %) and shows seasonal cycle of smaller amplitude than SAOZ. The satellites display a larger seasonality of the difference with SAOZ (mostly during winter with an amplitude of the bias  $0.5 \times 10^{15}$  molecules  $\text{cm}^{-2}$ ). At Reunion, the variations are similar to SCIAMACHY both versions.

In summary, satellite data, except GOME GDP5 and SCIAMACHY IUP, show less NO<sub>2</sub> during the convective season (from November to February in Bauru), a feature, which can be attributed to the “cloud-cover “ frequency (cf. Sect. 3.2). The noise generated by clouds in the NO<sub>2</sub> measurements is of lesser amplitude in the less cloudy Reunion Island, except on GOME IUP and OMI. A cloud filter has been applied on SCIAMACHY data in Bauru for characterizing the impact the clouds on the comparisons with SAOZ measurements (cf. Appendix A). From this analysis, the application of a cloud filtering results in a noise increase in the summer when clouds are more frequent and the number of satellite data reduced. However, there is no change in the

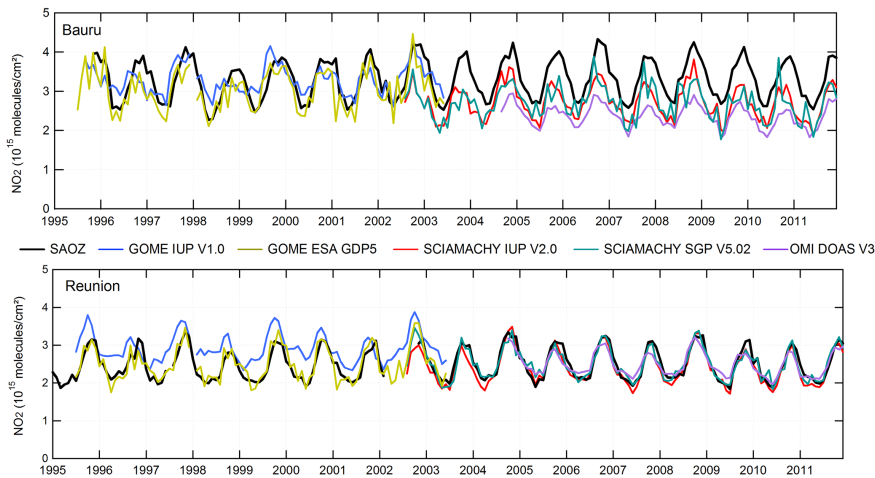


**Figure 13.** Satellite monthly mean NO<sub>2</sub> columns corrected to 90° AM over Bauru (top) and Reunion (bottom). GOME GDP5 (green), GOME IUP V1 (blue), SCIAMACHY IUP V2 (red), SCIAMACHY SGP5 (dark green), OMI DOAS V3 (purple). Time series of SAOZ at sunrise have been added in black.

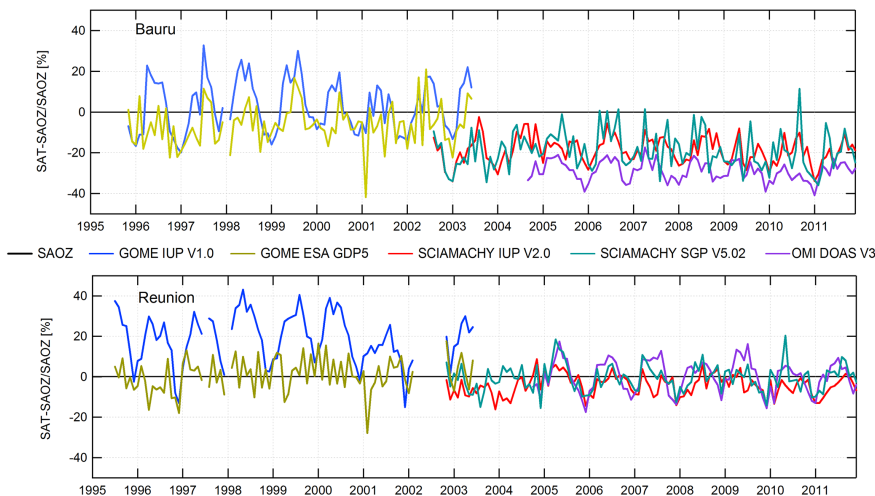


**Figure 14.** NO<sub>2</sub> relative mean difference of satellite data with SAOZ in % over Bauru (top) and Reunion (bottom). GOME GDP5 (green), GOME IUP V1 (blue), SCIAMACHY IUP V2 (red), SCIAMACHY SGP5 (dark green), OMI DOAS V3 (purple) and SAOZ sunrise (black).

NO<sub>2</sub> mean value showing that clouds have a limited impact on mean NO<sub>2</sub> column measurements.

The best satellite combination covering the full 1995–2011 SAOZ period are thus GOME GDP5 (1995–2002) and SCIAMACHY IUP V2 (2003–2011) showing smallest seasonality, requiring bias corrections of 6.3 % for GOME GDP5 and 18.8 % for SCIAMACHY IUP in Bauru and 0.8 and 4.1 % in Reunion for best matching with SAOZ.

#### 4.4 Merged satellite NO<sub>2</sub> series

Following this conclusion, a merged satellite composite series, displayed in Fig. 16, has been constructed with the GOME GDP5 (1995–2003) and SCIAMACHY IUP V2 (2003–2011) after normalization by addition of their

respective biases with SAOZ. As shown on the right of Fig. 16, the two series are highly correlated (0.89 in Bauru, 0.92 in Reunion) although more noisy over the first station and before 2003 with GOME GDP5 than afterwards with SCIAMACHY IUP. The two series show interannual variations out of phase with those of ozone (e.g., maximum instead of minimum during the El Niño event in 1997–1998). The seasonal variation of the difference between Bauru and Reunion seen by the satellites is similar to that reported by SAOZ (Fig. 17). Both show larger NO<sub>2</sub> by  $1.1 \times 10^{15}$  molecules cm<sup>-2</sup> (35 %) in the summer (January–March) due to NO<sub>x</sub> production by lightning, but still larger by  $0.6 \times 10^{15}$  molecules cm<sup>-2</sup> (18 %) in the winter, because, like ozone, the more southern equivalent latitude of Bauru

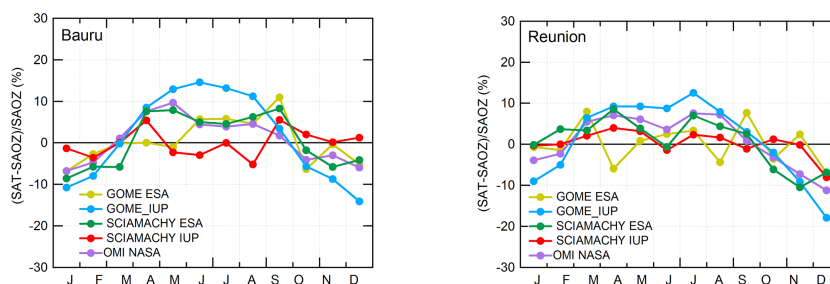


**Figure 15.** Relative difference of the NO<sub>2</sub> seasonal cycle between satellites and ground based observations at Bauru (left) and Reunion (right). GOME GDP5 (green), GOME IUP V1 (blue), SCIAMACHY IUP V2 (red), SCIAMACHY SGP5 (dark green), OMI DOAS V3 (purple).

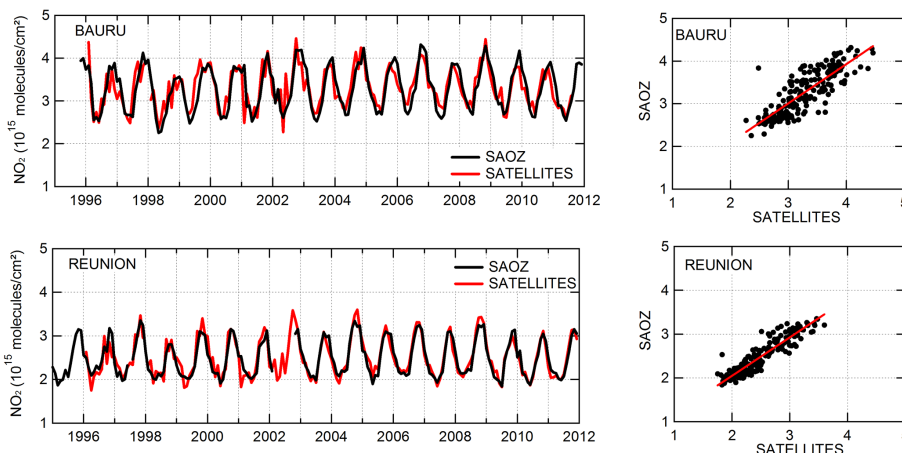


**Figure 16.** Left: SAOZ (black) and merged satellite (red) NO<sub>2</sub> columns ( $10^{15}$  molecules  $\text{cm}^{-2}$ ) in Bauru (top) and Reunion (bottom). Right: Correlation between SAOZ and merged satellite data ( $r^2 = 0.89$  in Bauru and  $r^2 = 0.92$  in Reunion).

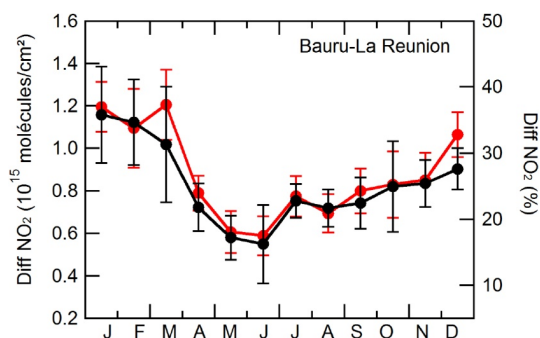


**Figure 17.** Seasonal cycle of the difference between Bauru and Reunion from SAOZ (black) and merged satellites (red).

compared to that of Reunion and the tropospheric pollution due to cane sugar burning.

In conclusion, there is excellent agreement between the merged satellite data set associating GOME GDP5 in the 1996–2003 period and SCIAMACHY IUP in the 2003–2011 period after correction for the NO<sub>2</sub> photochemical diurnal variation and respective biases, with the SAOZ series in the

southern tropics. Both show larger columns above the South American continent than over the SW Indian Ocean.

## 5 Conclusions

Long series of ground-based SAOZ-NDACC ozone and NO<sub>2</sub> total column observations at the southern tropics are available since 1995 in Bauru on the South American continent and since 1993 in Reunion Island in the Indian Ocean, providing a unique tool for evaluating the performances of the various satellite observations and building a reliable merged series for studying ozone and NO<sub>2</sub> trends since 1995. Since none of the satellites covers the full period, and systematic biases exist between them because of the many differences between instruments, wavelength ranges, absorption cross-sections and retrieval procedures, they require evaluation and bias corrections.

From comparisons with SAOZ, the best satellite data series for ozone in these regions are EP-TOMS (1995–2004) and OMI-TOMS (2005–2011), both confirming the larger ozone columns reported by SAOZ above South America continent compared to the Indian Ocean attributed to the ozone

production by lightning NO<sub>x</sub> in the upper troposphere in the summer and the import of ozone rich air from mid-latitudes in the lower stratosphere. The only difference found between satellites and SAOZ is the lower sensitivity of the latter to ozone-rich biomass-burning plumes in the mean troposphere.

The best satellite NO<sub>2</sub> measurements in the southern tropics are shown to be those of GOME GDP5 (1996–2003) and SCIAMACHY-IUP (2003–2011). Both of these measurements confirm, that ozone (the larger column seen by SAOZ above the South American continent) attributed to NO<sub>x</sub> production by frequent lightning in the summer and larger exchange of NO<sub>x</sub> rich air with the mid-latitudes in the winter in the lower stratosphere.

For both species, the most difficult piece in the satellite retrievals is the quantification of the tropospheric contribution frequently masked by high clouds in the tropics, particularly during the summer convective season.

Overall, the comparison of the data of the various satellites retrievals with the long series of ground-based SAOZ/NDACC observations allowed the creation of reliable merged satellite time-series for investigating, together with the SAOZ series, the possible trends and the origin of inter-annual variability of ozone and NO<sub>2</sub> in the southern tropics in the future.

### Appendix A: Impact of difference between satellite and SAOZ measurement location, surface layer pollution and clouds

A first issue in the construction of a merged satellite data series is the different orbit dependent location of satellite nadir observations and the location and local time of the zenith sky SAOZ measurements at twilight. For better coincidence observations, a procedure for selecting the data has been developed by Lambert et al. (2012), called optical path matching selection technique. The objective of the procedure is to reduce at best the noise in the difference between various observations generated by horizontal gradients or polluted areas. An example of the application of the method in the tropics is shown in Fig. A1, which is representing the NO<sub>2</sub> monthly mean % difference between SCIAMACHY IUP columns measured at 10h30 and corrected for the photochemical change (see Sect. 4.2) and SAOZ at sunrise in Bauru. The SCIAMACHY data, in black, are those of the overpass above the station (in a 200 km circle around the station), whereas the blue and green lines are the results of the optical path matching technique at the location of the summer solstice (in a 200 km circle around  $-23.12^{\circ}$  S;  $47.24^{\circ}$  W) and the winter solstice (in a 200 km circle around  $-21.6^{\circ}$  S;  $47.24^{\circ}$  W). All SCIAMACHY data present the same bias with SAOZ and the optical path matching data are noisier than the overpass. Therefore, when applying the optical path matching method in the tropics, the improvement is poor because of the small NO<sub>2</sub> (and O<sub>3</sub>) stratospheric columns gradients at this latitude and in addition, the noise in the data is increased because of the reduced number of co-located effective air masses. Furthermore, regarding the contribution of polluted events, the SAOZ zenith sky geometry at twilight makes the spectrometer less sensitive than nadir-viewing instruments to the lower levels. For ozone, the expected column increase in case of pollution at surface level is only 2 DU, (mixing ratio increase by 20 ppb at maximum), which has a negligible impact on monthly mean total columns. For NO<sub>2</sub>, the largest contribution is that of lightning NO<sub>x</sub> production at 10–15 km, which is seen by both SAOZ and nadir satellites. In addition, the near surface NO<sub>2</sub> contribution is reduced by photolysis during daytime, and is relatively small outside urban areas, explaining why polluted events have little impact on monthly mean differences between SAOZ and satellite data as shown in Fig. A1.

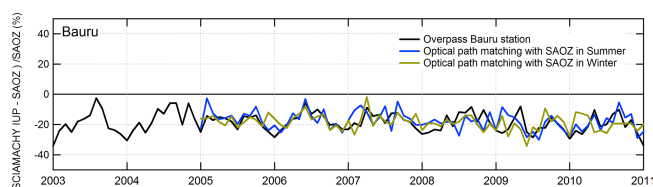


**Figure A1.** NO<sub>2</sub> percent mean difference between SCIAMACHY IUP and SAOZ over Bauru. SCIAMACHY overpass in black, Optical path matching in the solstice summer in blue and in the solstice winter in green.

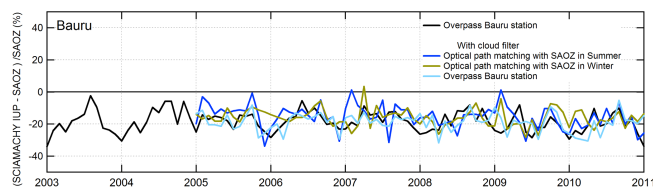


**Figure A2.** Same as Fig. A1 after removing days with cloud cover > 30%. Except during convective summer, cloud filtering has little impact on NO<sub>2</sub> monthly mean differences.

A second issue in the satellite–SAOZ comparison is that of the impact of frequent high altitude cirrus clouds and thunderstorm anvils in the tropics. This has been tested by applying a filter removing the data corresponding to a cloud cover greater than 30% using the SCIAMACHY cloud index. As shown in Fig. A2, this cloud filtering results in a larger noise in the summer NO<sub>2</sub> data because of the strong reduction of the number of observations, but has no clear impact on the NO<sub>2</sub> mean differences.

In conclusion, the limited O<sub>3</sub> and NO<sub>2</sub> column horizontal gradients, the small contribution of surface layer to the total columns outside urban areas, and the limited impact of the cloud masks, make the use of overpass nadir-viewing satellite measurements a reliable tool for long-term atmospheric composition changes studies in the tropics.

**Acknowledgements.** The authors thank the personnel of Reunion (J.-M. Metzger) and Bauru (B. Biazon and D. Quintao) stations for running the instruments. The SAOZ network is part of NDACC (Network for Detection of Atmospheric Composition Changes) supported by CNRS/INSU and CNES in France. The Reunion station is run in collaboration with the Observatoire de Physique Atmosphérique de la Réunion (OPAR) and University of La Réunion and that of Bauru with the Instituto de Pesquisas Meteorológicas of the University of Sao Paulo (IP-MET/UNESP) in Brazil, which are gratefully acknowledged. The satellite data are available through web access: TOMS (NASA) via the World Data Center for Remote Sensing of the Atmosphere (WDC/RSAT), Ozone Monitoring Instrument (NIVR/KNMI, FMI, NASA) via <http://avdc.gsfc.nasa.gov/> and HALOE via <http://haloe.gats-inc.com/home/index.php>. SCIAMACHY data extraction was carried out with a software tool developed by K. Bramstedt (University of Bremen). This work is part of M. Pastel PhD at the University P. and M. Curie (Paris 6) with the support of the French Ministry of Research and finalized with the support of the NORS/EU project (contract 284421).

Edited by D. Loyola



The publication of this article is financed by CNRS-INSU.

## References

- Balis, D., Lambert, J.-C., Van Roozendaal, M., Spurr, R., Loyola, D., Livschitz, Y., Valks, P., Amiridis, V., Gerard, P., Granville, J., and Zehner, C.: Ten years of GOME/ERS2 total ozone data The new GOME data processor (GDP) version 4. Ground-based validation and comparisons with TOMS V7/V8, *J. Geophys. Res.*, 112, D07307, doi:10.1029/2007JD009028, 2007.
- Bhartia, P. K. and Wellemeyer, C. W.: OMI TOMS-V8 Total O<sub>3</sub> Algorithm, Algorithm Theoretical Baseline Document: OMI Ozone Products, edited by: Bhartia, P. K., Vol. II, ATBD-OMI-02, Version 2.0, Aug. 2002.
- Boersma, K. F., Bucsela, E. J., Brinksma, E. J., and Gleason, J. F.: OMI algorithm theoretical basis document: OMI trace gas algorithms, vol. 4, edited by: Chance, K., Rep. ATBD-OMI-02, Goddard Space Flight Cent., NASA, Greenbelt, Md, 2002.
- Bogumil, K., Orphal, J., Homann, T., Voigt, S., Spietz, P., Fleischmann, O. C., Vogel, A., Hartmann, M., Bovensmann, H., Frerick, J., and Burrows, J. P.: Measurements of molecular absorption spectra with the SCIAMACHY Pre-Flight Model: Instrument characterization and reference spectra for atmospheric remote sensing in the 230–2380 nm region, *J. Photochem. Photobiol. A*, 157, 167–184, 2003.
- Bovensmann, H., Burrows, J. P., Buchwitz, M., Frerick, J., Noel, S., Rozanov, V. V., Chance, K. V., and Goede, A. P. H.: SCIAMACHY: Mission objectives and measurement modes, *J. Atmos. Sci.*, 56, 127–150, 1999.
- Bracher, A., Sinnhuber, M., Rozanov, A., and Burrows, J. P.: Using a photochemical model for the validation of NO<sub>2</sub> satellite measurements at different solar zenith angles, *Atmos. Chem. Phys.*, 5, 393–408, doi:10.5194/acp-5-393-2005, 2005.
- Bramstedt, K., Gleason, J., Loyola, D., Thomas, W., Bracher, A., Weber, M., and Burrows, J. P.: Comparison of total ozone from the satellite instruments GOME and TOMS with measurements from the Dobson network 1996–2000, *Atmos. Chem. Phys.*, 3, 1409–1419, doi:10.5194/acp-3-1409-2003, 2003.
- Buchard, V., Brogniez, C., Auriol, F., Bonnel, B., Lenoble, J., Tanskanen, A., Bojkov, B., and Veefkind, P.: Comparison of OMI ozone and UV irradiance data with ground-based measurements at two French sites, *Atmos. Chem. Phys.*, 8, 4517–4528, doi:10.5194/acp-8-4517-2008, 2008.
- Bucsela, E., Celarier, E., Wenig, M., Gleason, J., Veefkind, P., Boersma, K. F., and Brinksma, E.: Algorithm for NO<sub>2</sub> vertical column retrieval from the Ozone Monitoring Instrument, *IEEE Trans. Geosci. Remote Sens.*, 44, 1245–1258, doi:10.1109/TGRS.2005.863715, 2006.
- Burrows, J. P., Weber, M., Buchwitz, M., Rozanov, V., Ladstatter-Weißmayer, A., Richter, A., DeBeek, R., Hoogen, R., Bramstedt, K., Eichmann, K. U., Eisinger, M., and Perner, D.: The Global Ozone Monitoring Experiment (GOME): Mission Concept and First Scientific Results, *J. Atmos. Sci.*, 56, 151–175, 1999a.
- Burrows, J. P., Richter, A., Dehn, A., Deters, B., Himmelmann, S., Voigt, S., and Orphal, J.: Atmospheric Remote-sensing reference data from GOME – 2. Temperature-dependent absorption cross-sections of O<sub>3</sub> in the 231–794 nm range, *J. Quant. Spectrosc. Ra.*, 61, 509–517, 1999b.
- Celarier, E. A., Brinksma, E. J., Gleason, J. F., Veefkind, J. P., Cede, A., Herman, J. R., Ionov, D., Goutail, F., Pommereau, J.-P., Lambert, J.-C., Van Roozendaal, M., Pinardin, G., Wittrock, F., Schonhardt, Richter, A., Iranhim, O. W., Wagner, T., Bojkov, B., Mount, G., Spinei, E., Chen, C. M., Pongetti, T. J., Sander, S. P., Bucsela, E. J., Wenig, M. O., Swart, D. P. J., Volten, H., Kroon, M., and Levelt, P. F.: Validation of Ozone Monitoring Instrument nitrogen dioxide columns, *J. Geophys. Res.*, 113, D15S15, doi:10.1029/2007JD008908, 2008.
- Chipperfield, M. P.: Multiannual simulations with a three-dimensional chemical transport model, *J. Geophys. Res.*, 104, 1781–1805, 1999.
- Denis, L., Roscoe, H. K., Chipperfield, M. P., Van Roozendaal, M., and Goutail, F.: A new software suite for NO<sub>2</sub> vertical profile retrieval from ground-based zenith-sky spectrometers, *J. Quant. Spectrosc. Radiat. Trans.*, 92, 321–333, doi:10.1016/j.jqsrt.2004.07.030, 2005.
- Hauchecorne, A., Godin, S., Marchand, M., Hesse, B., and Souprayen, C.: Quantification of the transport of chemical constituents from the polar vortex to midlatitudes in the lower stratosphere using the high-resolution advection model MIMOSA and effective diffusivity, *J. Geophys. Res.*, 107, 8289, doi:10.1029/2001JD000491, 2002.
- Hendrick, F., Pommereau, J.-P., Goutail, F., Evans, R. D., Ionov, D., Pazmino, A., Kyrö, E., Held, G., Eriksen, P., Dorokhov, V., Gil, M., and Van Roozendaal, M.: NDACC/SAOZ UV-visible total ozone measurements: improved retrieval and comparison with correlative ground-based and satellite observations, *Atmos.*

- Chem. Phys., 11, 5975–5995, doi:10.5194/acp-11-5975-2011, 2011.
- Huntrieser, H., Schumann, U., Schlager, H., Höller, H., Giez, A., Betz, H.-D., Brunner, D., Forster, C., Pinto Jr., O., and Calheiros, R.: Lightning activity in Brazilian thunderstorms during TROC-CINOX: implications for NO<sub>x</sub> production, *Atmos. Chem. Phys.*, 8, 921–953, doi:10.5194/acp-8-921-2008, 2008.
- Ionov, D., Timofeyev, Y., Sinyakov, V., Semenov, V., Goutail, F., Pommereau, J.-P., Bucselá, E., Celarier, E., and Kroon, M.: Ground-based validation of EOS-Aura OMI NO<sub>2</sub> vertical column data in the mid-latitude mountain ranges of Tien Shan (Kyrgyzstan) and Alps (France), *J. Geophys. Res.*, 113, D15S08, doi:10.1029/2007JD008659, 2008.
- Lambert, J.-C. and Balis, D. S. (Eds.): Delta validation report for ERS-2 GOME data processor upgrade to version 4.0, Tech. Note ERSECLVL-EOPG-TN-04-0001, 82 pp., Eur. Space Agency, Paris, 2004.
- Lambert, J.-C., Van Roozendaal, M., De Maziere, M., Simon, P. C., Pommereau, J.-P., Goutail, F., Sarkissian, A., and Gleason, J. F.: Investigation of pole-to-pole performances of spaceborne atmospheric chemistry sensors with the NDSC, *J. Atmos. Sci.*, 56, 176–193, 1998.
- Lambert, J.-C., Granville, J., Van Roozendaal, M., Müller, J.-F., Goutail, F., Pommereau, J.-P., Sarkissian, A., Johnston, P. V., and Russell III, J. M.: Global Behavior of Atmospheric NO<sub>2</sub> as Derived from the Integrated Use of Satellite, Ground-based Network and Balloon Observations, in: *Atmospheric Ozone – 19th Quad. Ozone Symp.*, Sapporo, Japan, edited by: NASDA, 201–202, 2000.
- Lambert, J.-C., Koukouli, M., Balis, D., Granville, J., Lerot, C., and Van Roozendaal, M.: GOME/ERS-2–GDP5.0 upgrade of the GOME data processor for Improved total ozone columns–Validation Report, Tech. Note IASB-GOME-GDP5-VR, Eur. Space Agency, 2012.
- Levelt, P. F., Hilsenrath, E., Leppelmeier, G., Van Den Oord, G., Bhartia, P., Tamminen, J., Haan, J., and Veeffkind, J.: Science objectives of the Ozone Monitoring Instrument, *IEEE Trans. Geosci. Remote Sens.*, 44, 1199–1208, 2006.
- Lichtenberg, G., Bovensmann, H., Van Roozendaal, M., Doicu, A., Eichmann, K.-U., Hess, M., Hrechany, S., Kokhanovsky, A., Lerot, C., Noel, S., Richter, A., Rozanov, A., Schreier, F., and Tilstra, L. G.: SCIAMACHY Offline Level 1b-2 Processor ATBD (ENV-ATB-QWG-SCIA-0085, issue 1A), 2010.
- Loyola, D., Zimmer, W., Kiemle, S., Valks, P., and Pedergnana, M.: Product User Manual for GOME Total Columns of Ozone, NO<sub>2</sub>, tropospheric NO<sub>2</sub>, BrO, SO<sub>2</sub>, H<sub>2</sub>O, HCHO, OClO, and Cloud Properties, DLR/GOME/PUM/01, Iss./Rev. 2E, 2012.
- McPeters, R. D., Bhartia, P. K., Krueger, A. J., and Herman, J. R.: Earth Probe Total Ozone Mapping Spectrometer (TOMS) Data Products User's Guide, NASA Technical Publication 1998-206985, 64 pp., NASA Goddard Space Flight Center, Greenbelt, 1998.
- McPeters, R. D., Labow, G. J., and Logan, J. A.: Ozone climatological profiles for satellite retrieval algorithms, *J. Geophys. Res.*, 112, D05308, doi:10.1029/2005JD006823, 2007.
- Piters, A. J. M., Bramstedt, K., Lambert, J.-C., and Kirchhoff, B.: Overview of SCIAMACHY validation: 2002–2004, *Atmos. Chem. Phys.*, 6, 127–148, doi:10.5194/acp-6-127-2006, 2006.
- Platt, U.: Differential Optical Absorption Spectroscopy (DOAS), in: *Air Monitoring by Spectroscopic Techniques*, Chem. Anal. Ser., 127, edited by: Sigrist, M. W., 27–76, Wiley-Interscience, Hoboken, NJ, 1994.
- Pommereau, J.-P. and Goutail, F.: Ground-based measurements by visible spectrometry during Arctic Winter and Spring, *Geophys. Res. Lett.*, 15, 891–894, 1988.
- Pommereau, J.-P., Garnier, A., Borchi, F., and Nunes-Pinharanda, M.: Ozone and NO<sub>2</sub> zonal distribution in the tropical UTLS from SAOZ circum-navigating MIR balloon flights: relation to horizontal transport, convection and lightning, in: *Proc. XX Quad. Ozone Symp.*, edited by: Zerefos, C. S., 2, 1173–1174, 2004.
- Randriambelo, T., Baray, J.-L., and Baldy, S.: Effect of biomass burning, convective venting, and transport on tropospheric ozone over the Indian Ocean: Reunion Island field observations, *J. Geophys. Res.*, 105, 11813–11832, 2000.
- Richter, A. and Burrows, J. P.: Retrieval of Tropospheric NO<sub>2</sub> from GOME Measurements, *Adv. Space Res.*, 29, 1673–1683, 2002.
- Richter, A., Wittrock, F., Weber, M., Beirle, S., Kühl, S., Platt, U., Wagner, T., Wilms-Grabe, W., and Burrows, J. P.: GOME observations of stratospheric trace gas distributions during the splitting vortex event in the Antarctic winter 2002, Part I: Measurements, *J. Atmos. Sci.*, 62, 778–785, 2005.
- Richter, V., Eyring, J., Burrows, P., Bovensmann, H., Lauer, A., Sierk, B., and Crutzen, P. J.: Satellite Measurements of NO<sub>2</sub> from International Shipping Emissions, *Geophys. Res. Lett.*, 31, L23110, doi:10.1029/2004GL020822, 2004.
- Rivière, E. D., Maréchal, V., Larsen, N., and Cautenet, S.: Modelling study of the impact of deep convection on the UTLS air composition – Part 2: Ozone budget in the TTL, *Atmos. Chem. Phys.*, 6, 1585–1598, doi:10.5194/acp-6-1585-2006, 2006.
- Rozanov, A., Rozanov, V., Buchwitz, M., Kokhanovsky, A., and Burrows, J.: SCIATRAN 2.0 – A new radiative transfer model for geophysical applications in the 175–2400 nm spectral region, *Adv. Space Res.*, 36, 1015–1019, doi:10.1016/j.asr.2005.03.012, 2005.
- Russell, J. M. III, Gordley, L. L., Park, J. H., Drayson, S. R., Hesketh, D. H., Cicerone, R. J., Tuck, A. F., Frederick, J. E., Harries, J. E., and Crutzen, P.: The Halogen Occultation Experiment, *J. Geophys. Res.*, 98, 10777–10797, 1993.
- Spurr, R., Kurosu, T., and Chance, K.: A Linearized discrete Ordinate Radiative Transfer Model for Atmospheric Remote Sensing Retrieval, *J. Quant. Spectrosc. Radiat. Trans.*, 68, 689–735, 2001.
- Spurr, R., van Roozendaal, M., Loyola, D., Lerot, C., Van Geffen, J., Van Gent, J., Fayt, C., Lambert, J.-C., Zimmer, W., Doicu, A., Otto, S., Balis, D., Koukouli, M., and Zehner, C.: GDP 5.0 Upgrade of the GOME Data Processor for Improved Total Ozone Columns – Algorithm Theoretical Basis Document, DLR/GOME/ATBD/GDP5, Iss./Rev. 1B, 2012.
- Vandaele, A. C., Hermans, C., Simon, P. C., Carleer, M., Colin, R., Fally, S., Merienne, M.-F., Jenouvrier, A., and Coquart, B.: Measurements of the NO<sub>2</sub> absorption cross-section from 42000 cm<sup>-1</sup> to 10000 cm<sup>-1</sup> (238–1000nm) at 220 K and 294 K, *J. Quant. Spectrosc. Radiat. Trans.*, 59, 171–184, doi:10.1016/S0022-4073(97)00168-4, 1998.
- Vandaele, A. C., Fayt, C., Hendrick, F., Hermans, C., Humbled, F., Van Roozendaal, M., Gil, M., Navarro, M., Puentedura, O., Yela, M., Braathen, G., Stebel, K., Tornkvist, K., Johnston, P., Kreher, K., Goutail, F., Mieville, A., Pommereau, J.-P., Khaykin,

- S., Richter, A., Oetjen, H., Wittrock, F., Bugarski, S., Friez, U., Pfeilsticker, K., Sinreich, R., Wagner, T., and Corlett, G., and Leigh, R.: An intercomparison campaign of ground-based UV-visible measurements of NO<sub>2</sub>, BrO, and OCIO slant columns: Methods of analysis and results for NO<sub>2</sub>, *J. Geophys. Res.*, 110, D08305, doi:10.1029/2004JD005423, 2005.
- Van Roozendael, M., Loyola, D., Spurr, R., Balis, D., Lambert, J.-C., Livschitz, Y., Valks, P., Ruppert, T., Kenter, P., Fayt, C., and Zehner, C.: Ten years of GOME/ERS-2 total ozone data the new GOME data processor (GDP) version 4: 1. Algorithm description, *J. Geophys. Res.*, 111, D14311, doi:10.1029/2005JD006375, 2006.
- Van Roozendael, M., Spurr, R., Loyola, D., Lerot, C., Balis, D., Lambert, J.-C., Zimmer, W., van Gent, J., van Geffen, J., Koukouli, M., Granville, J., Doicu, A., Fayt, C., and Zehner, C.: Sixteen years of GOME/ERS-2 total ozone data: The new direct-fitting GOME Data Processor (GDP) version 5 – Algorithm description, *J. Geophys. Res.*, 117, D03305, doi:10.1029/2011JD016471, 2012.
- Vaughan, G., Roscoe, H., Bartlett, L. M., O'Connor, F. M., Sarkissian, A., Van Roozendael, M., Lambert, J.-C., Simon, P., Karlsen, K., Kastad Hoiskar, A., Fish, D., Jones, R., Freshwater, R., Pommereau, J.-P., Goutail, F., Andersen, S., Drew, D., Hughes, P., Moore, D., Mellqvist, J., Hegels, E., Klupfel, T., Erle, F., Pfeilsticker, K., and Platt, U.: An intercomparison of ground-based UV-visible sensors of ozone and NO<sub>2</sub>, *J. Geophys. Res.*, 102, 542–552, 1997.
- Veefkind, J. P., De Haan, J. F., Brinksma, E. J., Kroon, M., and Levelt, P. F.: Total ozone from the ozone monitoring instrument (OMI) using the DOAS technique, *IEEE T. Geosci. Remote*, 44, 1239–1244, 2006.
- Wellemeier, C. G., Bhartia, P. K., Taylor, S. L., Qin, W., and Ahn, C.: Version 8 Total Ozone Mapping Spectrometer (TOMS) Algorithm. C. Zerefos, technical note, 2004.
- Zipser, E., Cecil, D., Liu, C., Nesbitt, S., and Yorty, D.: Where are the most intense thunderstorms on Earth?, *Bull. Am. Meteor. Soc.*, 87, 1057–1071, 2006.